

Finite temperature pair density wave superconductivity in d -wave altermagnets

Amrutha N Madhusuthanan¹ and Madhuparna Karmakar^{1,*}

¹*Department of Physics and Nanotechnology, SRM Institute of Science and Technology, Kattankulathur, Chennai 603203, India*

(Dated: May 11, 2026)

We demonstrate that altermagnetism provides a field-free mechanism for stabilizing finite-momentum superconductivity in two dimensions. Using a non-perturbative static path approximation Monte Carlo approach, we show that a d -wave altermagnet supports a robust pair-density-wave (PDW) phase that persists over a finite temperature window despite strong thermal fluctuations. The underlying mechanism originates from momentum-dependent spin splitting, which effectively enhances pairing instabilities at finite center-of-mass momentum without Zeeman fields. We identify distinct thermal scales associated with phase coherence, gap closing, and pseudogap formation, and establish characteristic spectroscopic and real-space signatures of the PDW state. Our results reveal altermagnetism as a robust route to thermally stable finite-momentum superconductivity and provide experimentally testable signatures for altermagnetic materials.

Introduction: Finite momentum ($\mathbf{q} \neq 0$) superconductivity dates back to the Fulde–Ferrell–Larkin–Ovchinnikov (FFLO) [1, 2] and Sarma phases [3] in Pauli limited superconductors, wherein an applied Zeeman field induces imbalance in the fermionic population and promotes finite-momentum pairing instabilities [4–42]. In contrast, the pair density wave (PDW) represents a distinct class of spatially modulated superconducting (SC) states that can arise without spin imbalance, driven instead by electronic interactions and Fermi surface anisotropy [43–51]. Despite extensive theoretical work [44–51] and growing experimental evidence in systems such as Kagome metals [52, 53], UTe_2 [54, 55], $\text{EuRbFe}_4\text{As}_4$ [56], stabilizing PDW order at finite temperatures in two dimensions (2D) remains an open challenge due to its sensitivity to thermal fluctuations.

Altermagnetism (ALM) provides a natural route to finite-momentum pairing without external magnetic fields. Arising from magnetic space group symmetries, ALM generates momentum-dependent spin splitting without net magnetization [57–105], thereby mimicking a k -space Zeeman field that favors finite- \mathbf{q} pairing channels while avoiding orbital depairing effects. Previous theoretical studies, largely based on mean-field theory (MFT) and phenomenological approaches, have suggested that ALM can stabilize unconventional superconducting states including PDW [106–118]. However, whether such states remain stable against thermal fluctuations in 2D remains unresolved.

In this work, we address this issue using a non-perturbative static path approximated (SPA) Monte Carlo approach that captures thermal fluctuations of the pairing field. We show that a $d_{x^2-y^2}$ -wave altermagnet supports a robust PDW phase at zero magnetic field, persisting over a finite temperature window with appreciable phase coherence. The underlying mechanism is that momentum-dependent spin splitting selectively enhances finite-momentum pairing while suppressing the uniform superconducting channel. We map out the thermal phase diagram (Fig. 1) and identify distinct scales associated with phase coherence, gap closing, and pseudogap formation, establishing ALM as a viable route to thermally stable finite-momentum superconductivity in 2D.

Theoretical model: We model the system using the 2D at-

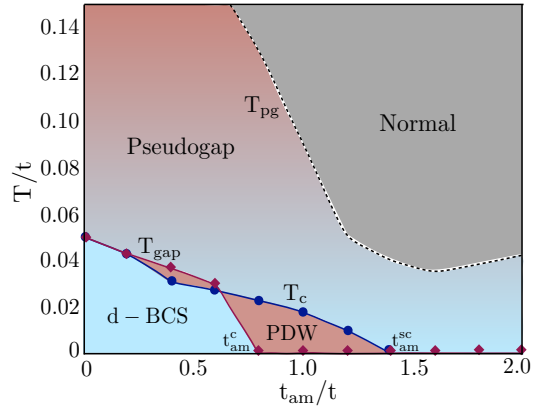


FIG. 1. Thermal phase diagram of d -wave ALM-SC in the $t_{am} - T$ plane showing the thermodynamic phases: (i) d -wave (uniform) BCS, (ii) PDW, (iii) pseudogap and (iv) normal, along with the corresponding thermal transition and crossover scales, T_c , T_{gap} and T_{pg} .

tractive Hubbard Hamiltonian with inter-site pairing and d -wave ALM interaction on a square lattice (see supplementary materials (SM) for the details), which reads as,

$$\hat{H} = \sum_{\langle ij \rangle, \sigma} (-t_{ij} + \sigma t_{am} \eta_{ij}) (\hat{c}_{i,\sigma}^\dagger \hat{c}_{j,\sigma} + h.c.) - \sum_{i,\sigma} (\mu + \sigma_i^z h) \hat{n}_{i,\sigma} - |U| \sum_{\langle ij \rangle} \hat{n}_i \hat{n}_j \quad (1)$$

where, $t_{ij} = t = 0.5$ is the nearest neighbor hopping and sets the reference energy scale of the system. The second term depicts the $d_{x^2-y^2}$ ALM interaction such that, t_{am} quantifies the strength of the interaction and η_{ij} is the d -wave form factor, with $t_{\hat{x}} = t - \frac{\sigma t_{am}}{2}$ and $t_{\hat{y}} = t + \frac{\sigma t_{am}}{2}$; $\sigma = +(-)$ for the $\uparrow(\downarrow)$ spin species. d -wave SC pairing is brought in via the effective attractive interaction $|U| > 0$ (see SM), the chemical potential μ dictates the fermionic number density in the system and the Zeeman field $h \neq 0$ allows for a population imbalance between the fermionic species, leading to finite magnetization, m . The model is made numerically tractable via Hubbard-Stratonovich (HS) [119, 120] decomposition of the

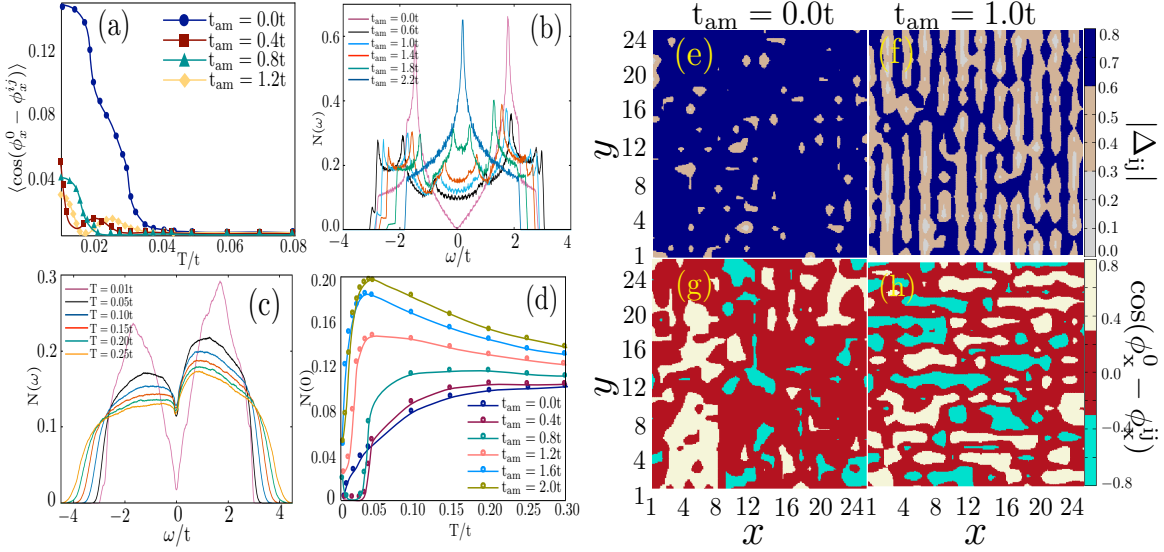


FIG. 2. Spectroscopic and thermodynamic indicators at representative $t_{am} - T$ cross sections quantifying the BCS and PDW regimes. (a) Temperature dependence of average SC phase correlation ($\langle \cos(\phi_x^0 - \phi_x^{ij}) \rangle$) (ϕ_x^0 represents the SC phase at a reference site), (b) single particle DOS ($N(\omega)$) at $T = 0.01t$ (as obtained for $L = 100$ using variational MFT), (c) temperature dependence of the single particle DOS at $t_{am} = 1.0t$ showing thermal evolution of the pseudogap phase, (d) temperature dependence of the spectral weight at the Fermi level ($N(0)$) at representative t_{am} 's, (e)-(f) real space maps showing the pairing field amplitude $|\Delta_{ij}|$ at $t_{am} = 0.0t$ (BCS) and $t_{am} = 1.0t$ (PDW), respectively for $T = 0.02t$, (g)-(h) the corresponding phase correlations ($\cos(\phi_x^0 - \phi_x^{ij})$). Note the uniaxial spatial modulations in the pairing field amplitude and phase correlation salient to the PDW phase. The spatial maps correspond to a single Monte Carlo snapshot.

four-fermion interaction term, introducing random fluctuating complex (bosonic) auxiliary field $\Delta_{ij} = |\Delta_{ij}|e^{i\phi_{ij}}$ which couples to the d -wave pairing singlet, $(c_{j\uparrow}c_{j\downarrow} + c_{j\downarrow}c_{i\downarrow})$. The pairing field amplitude is quantified by $|\Delta_{ij}|$ and $\phi_{ij} \in \{\phi_{ij}^x, \phi_{ij}^y\}$ corresponds to the momentum dependent SC phase with the relative phase being $\phi_{ij}^{rel} = \phi_{ij}^x - \phi_{ij}^y$ [16, 17].

Our primary numerical approach SPA is based on the adiabatic approximation of the slow (thermal) bosonic field serving as a random, static disordered, fluctuating background to the fast moving fermions [121–124]. The approximation allows one to treat the bosonic field as a classical variable, provides access to real frequency dependent quantities without requiring an analytic continuation and provides reliable estimates of the thermal scales (see SM). For the ground state, SPA is supplemented by a variational MFT with the SC pairing field amplitude and pairing momenta serving as suitable variational parameters for optimization of the free energy (see SM).

The thermodynamic phases and transition scales are quantified in terms of: (i) mean SC phase correlation ($\langle \cos(\phi_x^0 - \phi_x^{ij}) \rangle$), (ii) (spin-resolved) single particle density of states, DOS ($N^\sigma(\omega)$), (iii) spectral gap at the Fermi level (E_g), (iv) magnetization (m), (v) real space maps corresponding to SC pairing field amplitude ($|\Delta_{ij}|$) and phase correlation ($\cos(\phi_x^0 - \phi_x^i)$) and (vi) (spin-resolved) low energy spectral weight distribution mapping out the Fermi surface topology ($A^\sigma(\mathbf{k}, 0)$) (see SM). SPA Monte Carlo is carried out at $U = -4t$ in the grand canonical ensemble with $\mu = -0.2t$ cor-

responding to a fermionic number density of $n \approx 0.9$; on a system size of $L = 24$, unless specified otherwise.

PDW at $T \neq 0$: Fig.1 shows the thermal phase diagram of the system in the $t_{am} - T$ plane, characterized based on the thermodynamic and spectroscopic signatures presented in Fig.2. Fig.2(a-d) respectively quantify phase coherence, gap closing and pseudogap formation. The thermodynamic phases are broadly classified based on the pairing field amplitude and momentum into: (i) d -wave BCS ($|\Delta_{ij}| \neq 0$, $\mathbf{q} = 0$), (ii) collinear PDW ($|\Delta_{ij}| \neq 0$, $\mathbf{q} \in \{0, \pi\}$) and (iii) pseudogap ($|\Delta_{ij}| \rightarrow 0$, $\mathbf{q} = 0$), demarcated primarily by three thermal scales viz. T_c , which quantifies the loss of (quasi) long range global SC phase coherence via a second order phase transition, T_{gap} , signifying the collapse of E_g at the Fermi level and T_{pg} , which maps out the thermal crossover scale between the short range phase correlated and the non-SC phases. Note that T_c corresponds to the Berezinskii-Kosterlitz-Thouless temperature depicting the algebraic decay of the SC phase correlations.

The d -wave BCS state is typified by a uniform $d_{x^2-y^2}$ SC pairing with (quasi) long range phase coherence; at $t_{am} = 0.0t$ the global SC phase coherence is lost at $T_c \sim 0.05t$ (Fig.2(a)). t_{am} results in monotonic suppression of the T_c leading to a critical $t_{am}^{sc} \approx 1.4t$ quantifying the loss of global SC order, at $T = 0.01t$ (ground state). The single particle DOS at $t_{am} = 0.0t$ (as obtained via variational MFT calculations at $T = 0.01t$) exhibiting $N(\omega) \propto \omega$ as $\omega \rightarrow 0$ in Fig.2(b), signifies the purely nodal SC gap structure salient to the d -wave

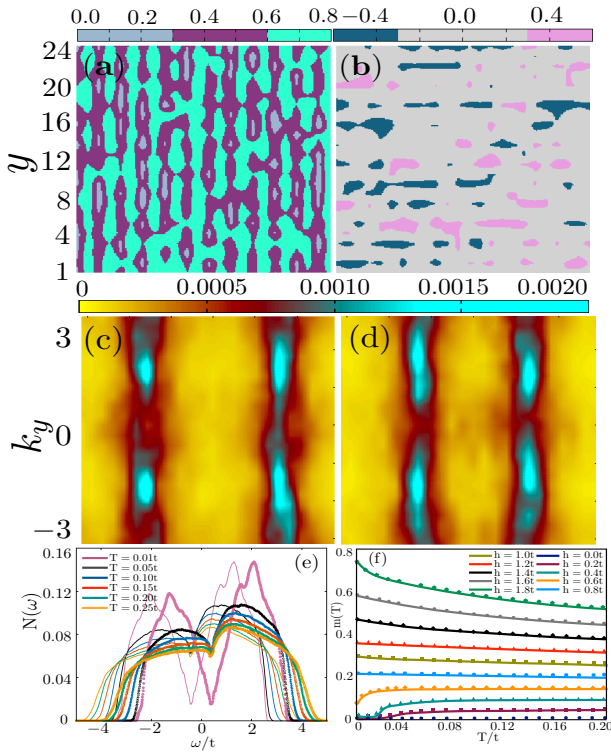


FIG. 3. Thermodynamic and spectroscopic signatures at $h = 0.4t$ and $t_{am} = 1.0t$, representing the 1D-LO phase. (a)-(b) Show the real space maps corresponding to the pairing field amplitude and phase correlation; spin-resolved Fermi surface topology at $T = 0.02t$, determined based on the low energy spectral weight distribution at the Fermi level as, (c) $A^{\uparrow}\mathbf{k}, 0$ and (d) $A^{\downarrow}\mathbf{k}, 0$; (e) thermal evolution of the spin-resolved single particle DOS with the Zeeman field shifted Fermi level at $\omega = \pm h$ (\uparrow -spin is represented by solid curves and \downarrow -spin is represented by points), (f) temperature dependence of magnetization ($m(T)$) at selected h demarcating the PDW and 1D-LO phases.

BCS phase.

The BCS to PDW transition is of second order; along with a suppressed T_c scale the $\mathbf{q} \neq 0$ PDW phase is characterized by a gapless low temperature single particle spectra comprising of in-gap states and additional van Hove singularities, as shown in Fig.2(b). The origin of the in-gap states is due to the finite momentum scattering of the quasiparticles. In contrast to the d -wave BCS phase the $|\mathbf{k}_{\uparrow}\rangle$ state in PDW connects to the $|\mathbf{k} + \mathbf{q}_{\uparrow}\rangle$ and $|\mathbf{k} - \mathbf{q}_{\downarrow}\rangle$ states in addition to $|\mathbf{k}_{\downarrow}\rangle$, giving rise to multiple branches and additional van-Hove singularities in the electronic dispersion spectra. The in-gap states lead to the transition between the gapped (d -wave BCS) and gapless (PDW) SC phases and quantify the thermal scale T_{gap} ; the corresponding critical ALM interaction at $T = 0.01t$ is marked as $t_{am}^c \approx 0.8t$. t_{am} promotes the in-gap states over the regime $t_{am}^c < t_{am} \lesssim t_{am}^{sc}$, such that, for $t_{am} > t_{am}^{sc}$ the SC correlations are lost and the single particle DOS mimics the non-interacting spectra.

The thermal evolution of the single particle DOS as ob-

tained based on SPA is shown in Fig.2(c) at the selected ALM interaction of $t_{am} = 1.0t$, representing deep in the PDW regime. The low temperature phase is gapless with finite spectral weight at the Fermi level and prominent coherence peaks at the gap edges. Note that in contrast to MFT (Fig.2(b)) thermal fluctuations tend to smooth out the in-gap features. Increase in temperature progressively accumulates spectral weight at the Fermi level and broadens the coherence peaks via large transfer of spectral weight away from the Fermi level, characterizing the pseudogap phase where the short range SC correlations dominate the physics. For $T \gtrsim 0.12t$ the spectral weight at the Fermi level begins to deplete with temperature demarcating the thermal crossover scale T_{pg} between the pseudogap and the non-SC phases. T_{pg} is quantified in Fig.2(d), wherein the spectral weight at the Fermi level ($N(0)$) is shown as a function of temperature at selected t_{am} 's and T_{pg} marks the temperature at which $dN(0)/dT$ becomes nearly independent of temperature.

The non-trivial spectroscopic signatures across the BCS-PDW transition leave its imprint on the underlying Fermi surface topology. While the nodal architecture of the $d_{x^2-y^2}$ pairing is observed at $t_{am} = 0.0t$ with large spectral weight at point nodes, the PDW phase is characterized in terms of line nodes, in semblance with the collinear spatial modulation of the SC correlations (see SM).

We sum up the thermodynamic signatures of the finite temperature PDW phase in Fig.2(e-h) in terms of the real space maps corresponding to the SC pairing field amplitude and phase correlation at $t_{am} = 1.0t$ and $T = 0.02t$ (Fig.2(f) and (h)), and compare the same with those in the d -wave BCS phase at $t_{am} = 0.0t$ (Fig.2(e) and (g)). In sharp contrast with the uniform, (quasi) long range phase coherent d -wave BCS phase the PDW regime shows prominent uniaxial modulations in the real space both in $|\Delta_{ij}|$ and $\cos(\phi_0^x - \phi_i^x)$. The observation constitutes direct (numerical) evidence of a stable PDW phase at finite temperatures, within a fluctuation framework.

Effect of Zeeman field: The order parameter that quantifies the second order phase transition between the PDW and a Zeeman field controlled FFLO phase at low temperatures is magnetization, with the FFLO phase characterized by $m \neq 0$ and an imbalance in the population of the fermionic species. In Fig. 3 we analyze the (uniaxial) 1D-LO phase in terms of its thermodynamic and spectroscopic signatures at a representative Zeeman field of $h = 0.4t$ and $t_{am} = 1.0t$, at $T = 0.02t$. The real space modulation in the SC pairing field amplitude and phase correlation, akin to the PDW phase are presented in Fig.3(a) and Fig.3(b). The mismatch in the Fermi surface topology arising out of the moderate imbalance in the spin dependent fermionic population can be seen from Fig.3(c) and Fig.3(d). Stronger h results in larger imbalance in the fermionic populations and leads to (biaxial) 2D-LO phase (see SM). Our MFT results show that at the ground state, the h controlled phases and phase transitions are demarcated in terms of two critical fields h_{c1} and h_{c2} , such that, the transition across h_{c1} between the 1D-LO and 2D-LO is of first order while the 2D-LO gives way to a polarized Fermi liquid (PFL) devoid of

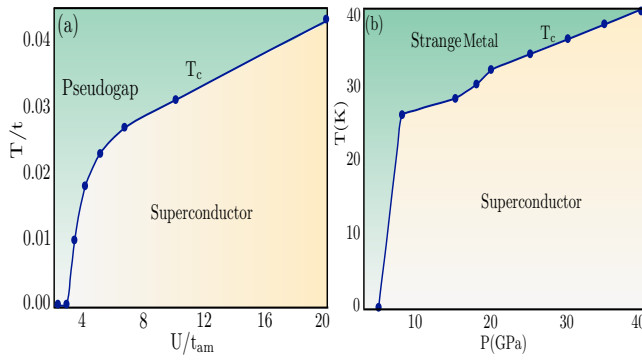


FIG. 4. (a) Thermodynamic phases in the effective interaction-temperature ($U/t_{am} - T$) plane demarcating the superconductor and pseudogap phases via the SC transition scale T_c . The effective interaction (U/t_{am}) mimics the applied pressure in terms of the reconstruction of the electronic band structure. (b) Pressure induced SC phase transition in CsV₂Se₂O and the corresponding T_c , as observed through transport measurements [125].

any SC correlations via a second order phase transition across h_{c2} (see SM). We observe that the LO phase (particularly, 2D-LO) is fragile as compared to the PDW with rapid suppression in its T_c w. r. t. the applied Zeeman field such that, for $h = 1.0t$ the (quasi) long range LO correlations are destroyed for $T \gtrsim 0.005t$ (see SM). This establishes that stability of the PDW phase is intrinsic to ALM, not generic to finite- \mathbf{q} pairing.

Thermal evolution of the spin resolved single particle DOS at $h = 0.4t$ and $t_{am} = 1.0t$ is shown in Fig.3(e). The applied Zeeman field shifts the Fermi level as $\omega = \pm h$ with a significant spectral weight at the Fermi level even at low temperatures; the SC state is therefore gapless. Thermal fluctuations transfer spectral weight away from the Fermi level and defines the pseudogap regime marked by short range SC correlations bounded by the thermal scale T_{pg} . Temperature dependence of magnetization at selected h values for $t_{am} = 1.0t$ that distinguishes the LO from the PDW phase is shown in Fig.3(f). The PDW phase ($h = 0.0t$) lacks a net magnetization and for $h \neq 0$ the point of inflection of the $m(T)$ curve marks the onset of the LO phase. Magnetization in the high temperature PFL (non SC) regime is independent of T . Magnetization and SC correlations are complementary to each other in the LO phase and the spatial maps depict the same (see SM).

Discussion and conclusions: We demonstrated that ALM provides a field-free mechanism for stabilizing PDW superconductivity at finite temperatures in 2D, overcoming the conventional fragility of finite-momentum pairing in low dimensions. The intrinsic momentum-dependent spin splitting in altermagnets acts as an effective k -space Zeeman field, selectively enhancing pairing at finite center-of-mass momentum while suppressing uniform superconductivity. In contrast to Zeeman-field-induced FFLO states, which are rapidly suppressed by thermal fluctuations, the ALM route yields a qual-

itatively more stable finite-momentum superconducting state.

PDW has been extensively discussed in the context of the pseudogap phase and competing orders in high- T_c cuprates [126–133]. For ALM materials, experimental evidence of PDW superconductivity continues to be lacking, though there are prospective candidates such as, Kagome superconductors AV₃Sb₅ ($A = K, Cs$) [52, 53, 134]. Recent transport measurements on the ALM material, alkali vanadium oxychalcogenide CsV₂Se₂O brought forth a pressure induced d -wave SC state, originating from a density-wave parent state [125]. It was further shown that the high temperature phase of this system comprise of a strange metal (pseudogap) phase with suppressed SC correlations, as shown in Fig.4(b). For a model Hamiltonian, the electronic band structure changes arising due to an applied pressure can be modelled in terms of effective electronic interaction. As a function of ALM interaction we define a parameter as, $U_{eff} = U/t_{am}$ such that, the effective fermionic interaction is dictated by the ALM coupling. The corresponding thermal phase diagram mapping out the T_c is shown in Fig.4(a) and suggests reasonable qualitative agreement with the experimental observations.

PDW correlations with d -wave symmetry are highly susceptible to thermal fluctuations, making their stability in 2D challenging. Standard non-perturbative methods cannot access sufficiently low temperatures, while MFT overestimates PDW stability at both $T = 0$ and finite T (see SM). Our approach overcomes these limitations and provides quantitative estimates of thermal transition and crossover scales in a d -wave ALM-superconductor, establishing finite-temperature PDW stability. The method has been widely applied to many-body systems, including unconventional superconductors [4, 5], frustrated lattices and Mott transitions [135, 136], flat and multiband systems [124, 137, 138], and altermagnetic metals [139]. It captures thermal fluctuations but neglects quantum fluctuations, reducing to MFT as $T \rightarrow 0$. The dominant low-energy fluctuations arise from the $U(1)$ phase, with lattice effects gapping translational and rotational modes, leaving XY -type excitations. While comparison with determinant quantum Monte Carlo remains unavailable for ALM systems, our results are reliable within SPA for $T > T_{FL}$, where T_{FL} corresponds to the Fermi liquid coherence temperature [121–124]. Overall, ALM provides a robust route to stabilizing finite-momentum superconductivity without external fields in 2D.

Acknowledgment: M.K. would like to acknowledge the use of the high performance computing facility (AQUA) at the Indian Institute of Technology, Madras, India. MK acknowledges the support from Anusandhan National Research Foundation (ANRF), Govt. of India through the grant ANRF/ARG/2025/001620.

SUPPLEMENTARY INFORMATION

Model Hamiltonian and d -wave pairing: An attractive fermionic interaction doesn't lead to an inter-site pairing by itself. If we start with a repulsive Hubbard model the s -wave pairing is inhibited by the formation of the local moments. In the strong coupling regime a $t - J$ model obtains from the repulsive Hubbard model if the double occupancy is projected out as [16, 17],

$$\hat{H} = \mathcal{P} \left[\sum_{\langle ij \rangle, \sigma} t_{ij} (\hat{c}_{i,\sigma}^\dagger \hat{c}_{j,\sigma} + h.c.) + \sum_{ij} J_{ij} (\vec{\sigma}_i \cdot \vec{\sigma}_j - \frac{1}{4} \hat{n}_i \hat{n}_j) - \mu N \right] \mathcal{P} \quad (2)$$

where, \mathcal{P} is the projection operator that eliminates the double occupancy, $J_{ij} = 4t_{ij}^2/U$ and $\vec{\sigma}$ is the electron spin operator. The Hamiltonian now contains spin-spin and density-density coupling but the projection needs to be retained for further calculation. An alternate approach can be implemented wherein both the Hubbard and the inter-site interactions are retained. The resulting $t - J - V$ model doesn't require explicit projection and the corresponding Hamiltonian reads as,

$$\hat{H} = \sum_{\langle ij \rangle, \sigma} (-t_{ij} + \sigma t_{am} \eta_{ij}) (\hat{c}_{i,\sigma}^\dagger \hat{c}_{j,\sigma} + h.c.) - |U| \sum_{\langle ij \rangle} \hat{n}_i \hat{n}_j + V \sum_i \hat{n}_{i\uparrow} \hat{n}_{i\downarrow} - \mu N \quad (3)$$

where, we have taken into account the spin-dependent ALM interaction such that, t_{am} quantifies the strength of the interaction and η_{ij} is the d -wave form factor, leading to $t_{\hat{x}} = t - \frac{\sigma t_{am}}{2}$ and $t_{\hat{y}} = t + \frac{\sigma t_{am}}{2}$; $\sigma = +(-)$ for the $\uparrow(\downarrow)$ spin species. We treat U and V independently and consider the $V = 0$ limit such that, the local moment formation is completely suppressed. The resulting Hamiltonian includes density-density coupling which can be decomposed into bosonic auxiliary pairing field Δ_{ij} as follows:

The partition function of the system is written in the functional integral form in terms of the Grassmann fields $\psi_{i\sigma}(\tau)$ and $\bar{\psi}_{i\sigma}(\tau)$,

$$\begin{aligned} Z &= \int \mathcal{D}\psi \mathcal{D}\bar{\psi} \exp \left\{ - \int_0^\beta d\tau \mathcal{L}(\tau) \right\} \\ \mathcal{L}(\tau) &= \mathcal{L}_0(\tau) + \mathcal{L}_U(\tau) \\ \mathcal{L}_0(\tau) &= \sum_{\langle ij \rangle, \sigma} \{ \bar{\psi}_{i\sigma} ((\partial_\tau - \mu - \sigma_i^z h) \delta_{ij} + t_{ij} - \sigma t_{am} \eta_{ij}) \psi_{j\sigma} \} \\ \mathcal{L}_U(\tau) &= -U \sum_{\langle ij \rangle, \sigma \sigma'} \bar{\psi}_{i\sigma} \psi_{i\sigma} \bar{\psi}_{j\sigma'} \psi_{j\sigma'} \end{aligned} \quad (4)$$

where, $t_{ij} = t = 0.5$ is the nearest neighbor hopping and sets the reference energy scale of the system. Superconducting pairing is brought in via the attractive interaction $|U| > 0$, the chemical potential μ dictates the fermionic number density in the system and the Zeeman field h allows for a population imbalance between the fermionic species, leading to a finite magnetic polarization, m . β is the inverse temperature.

We decompose the interaction term using Hubbard Stratonovich (HS) decomposition [119, 120] introducing the bosonic auxiliary d -wave pairing singlet $\Delta_{ij}(\tau)$. Here ij and τ refer to the spatial and imaginary time dependence of the pairing field, respectively. In terms of the Matsubara frequency $\Omega_n = 2\pi nT$ the pairing field reads as, Δ_{ijn} , where T is temperature. The resulting partition function is given as,

$$\begin{aligned} Z &= \int \mathcal{D}\psi \mathcal{D}\bar{\psi} \mathcal{D}\Delta \mathcal{D}\Delta^* e^{-\int_0^\beta d\tau \mathcal{L}(\tau)} \\ \mathcal{L}(\tau) &= \mathcal{L}_0(\tau) + \mathcal{L}_U(\tau) + \mathcal{L}_{cl}(\tau) \\ \mathcal{L}_0(\tau) &= \sum_{\langle ij \rangle, \sigma} \{ \bar{\psi}_{i\sigma} ((\partial_\tau - \mu - \sigma_i^z h) \delta_{ij} + t_{ij} - \sigma t_{am} \eta_{ij}) \psi_{j\sigma} \} \\ \mathcal{L}_U(\tau) &= - \sum_{i \neq j} \Delta_{ij} (\bar{\psi}_{i\uparrow} \bar{\psi}_{j\downarrow} + \bar{\psi}_{j\uparrow} \bar{\psi}_{i\downarrow}) + h.c. \\ \mathcal{L}_{cl}(\tau) &= 4 \sum_{i \neq j} \frac{|\Delta_{ij}|^2}{|U|} \end{aligned} \quad (5)$$

The fermions are now quadratic but at the cost of an extra integral over Δ and Δ^* . The $\int \mathcal{D}\psi \mathcal{D}\bar{\psi}$ integral can now be performed to generate the effective action for the random background fields $\{\Delta\}$,

$$\begin{aligned} Z &= \int \mathcal{D}\Delta \mathcal{D}\Delta^* e^{-S_{eff}(\Delta, \Delta^*)} \\ S_{eff} &= \ln \text{Det}[\mathcal{G}^{-1}\{\Delta, \Delta^*\}] + \int_0^\beta d\tau \mathcal{L}_{cl}(\tau) \end{aligned} \quad (6)$$

here, \mathcal{G} is the electronic Green's function in the $\{\Delta\}$ background.

SPA Monte Carlo: Within the framework of SPA, the auxiliary field retains the spatial fluctuations at all orders but retains only the $\Omega_n = 0$ mode of the Matsubara frequency, such that, $\Delta_{ij}(\tau) \rightarrow \Delta_{ij}$. The system can be thought of as fermions moving on a random correlated background of classical Δ_{ij} . The resulting effective Hamiltonian reads as,

$$\begin{aligned} H_{eff} &= \sum_{\langle ij \rangle, \sigma} (-t_{ij} + \sigma t_{am} \eta_{ij}) (c_{i\sigma}^\dagger c_{j\sigma} + h.c.) \\ &+ \sum_{i \neq j} \Delta_{ij} (c_{i\uparrow}^\dagger c_{j\downarrow}^\dagger + c_{j\uparrow}^\dagger c_{i\downarrow}^\dagger) + h.c. - \mu \sum_{i,\sigma} \hat{n}_{i,\sigma} \\ &- h \sum_{i,\sigma} \sigma_i^z \hat{n}_{i,\sigma} + 4 \sum_{i \neq j} \frac{|\Delta_{ij}|^2}{|U|} \end{aligned} \quad (8)$$

where, the last term corresponds to the stiffness cost associated with the now classical auxiliary field.

The $\{\Delta_{ij}\}$ background obeys the Boltzmann distribution, $P\{\Delta_{ij}\} \propto \text{Tr}_{c,c^\dagger} e^{-\beta H_{eff}}$, related to the free energy of the system. For large, random background the trace is taken numerically. The background configurations are generated by Monte Carlo simulation, diagonalizing H_{eff} for each attempted update of Δ_{ij} . The computation cost is brought down by implementing traveling cluster approximation (TCA) scheme [16, 17]. The required fermionic correlators are then computed on the optimized background configurations.

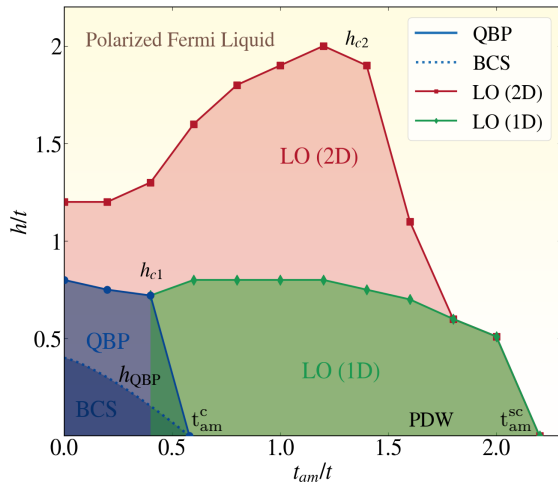


FIG. 5. Ground state phase diagram of d -wave altermagnetic superconductor in the $t_{am} - h$ -plane showing the BCS, QBP, PDW, LO and PFL phases along with the corresponding transition scales (solid lines with points).

SPA benchmarks: The Static Path Approximation (SPA) has been widely employed to investigate a broad range of quantum many-body phenomena. These include the BCS–BEC crossover in superconductors [140], Fulde–Ferrell–Larkin–Ovchinnikov (FFLO) superconductivity in both solid-state systems and ultracold atomic gases [141, 142], Mott transitions in frustrated lattices [143–147], d -wave superconductivity [148], the coexistence and competition between magnetic and d -wave superconducting orders [149], orbital-selective magnetism relevant to iron-based superconductors [150], and strain-driven superconductor–insulator transitions in flat-band systems [137], among others.

In many of these contexts, numerically exact techniques such as Determinant Quantum Monte Carlo (DQMC) become impractical due to limitations arising from the sign problem or finite system sizes, particularly in multiband settings. Consequently, controlled approximations are essential. Within this framework, SPA provides a robust and computationally efficient approach, enabling accurate characterization of low-temperature phases as well as the thermal properties of strongly correlated systems.

Observables: The ground state and finite temperature phases are characterized based on the following thermodynamic and spectroscopic signatures,

- Phase correlation, The x -component of the phase correlation is defined as,

$$\langle \cos(\phi_x^0 - \phi_x^{ij}) \rangle = \frac{1}{N} \langle \sum_{i \neq j} \cos(\phi_x^0 - \phi_x^{ij}) \rangle \quad (9)$$

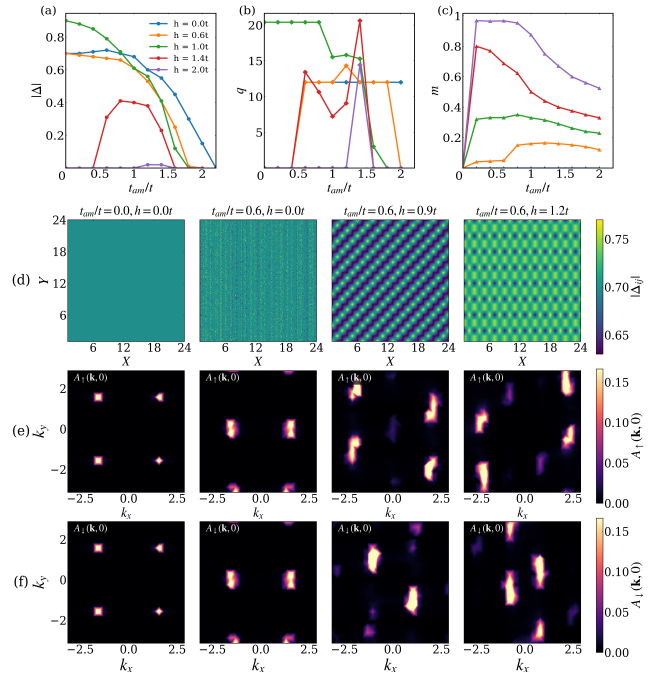


FIG. 6. Mean field estimates of the thermodynamic and spectroscopic quantities at selected $t_{am} - h$ cross sections. (a) Pairing field amplitude ($|\Delta|$), (b) pairing momentum ($q = \sqrt{q_x^2 + q_y^2}$), (c) magnetic polarization (m), (d) real space maps of the pairing field amplitude at representative fields corresponding to BCS, PDW, 1D-LO and 2D-LO phases, (e-f) spin resolved low energy spectral weight distribution ($A_\sigma(\mathbf{k}, 0)$) mapping out the underlying Fermi surface.

- Magnetization,

$$m = \frac{1}{N} \langle \sum_i (n_{i\uparrow} - n_{i\downarrow}) \rangle \quad (10)$$

- Single particle DOS,

$$N(\omega) = \langle \frac{1}{N} \sum_i (|u_n^i|^2 \delta(\omega - E_n) + |v_n^i|^2 \delta(\omega + E_n)) \rangle \quad (11)$$

- Spin resolved low energy spectral weight distribution,

$$A_\sigma(\mathbf{k}, 0) = -(1/\pi) \text{Im} G_\sigma(\mathbf{k}, \omega \rightarrow 0) \quad (12)$$

where, i and j correspond to two different sites on the lattice. $\langle \cdot \rangle$ corresponds to thermal average. $n_{i\sigma}$ are the number of the individual fermionic species, while u_n^i and v_n^i are Bogoliubov eigenfunctions corresponding to the eigenvalue E_n . The single particle Green's function reads as, $G(\mathbf{k}, \omega) = \lim_{\delta \rightarrow 0} G(\mathbf{k}, i\omega_n)|_{i\omega_n \rightarrow \omega + i\delta}$, where $G(\mathbf{k}, \omega)$ is the imaginary frequency transform of $\langle c_{\mathbf{k}}(\tau) c_{\mathbf{k}}^\dagger(0) \rangle$.

Variational MFT calculation: As $T \rightarrow 0$, the thermal fluctuations die off and suitable trial solutions can be proposed for the SC state in terms of the pairing field amplitude $|\Delta_{ij}|$ and the pairing momentum $q \in \{q_x, q_y\}$, which can then be used as

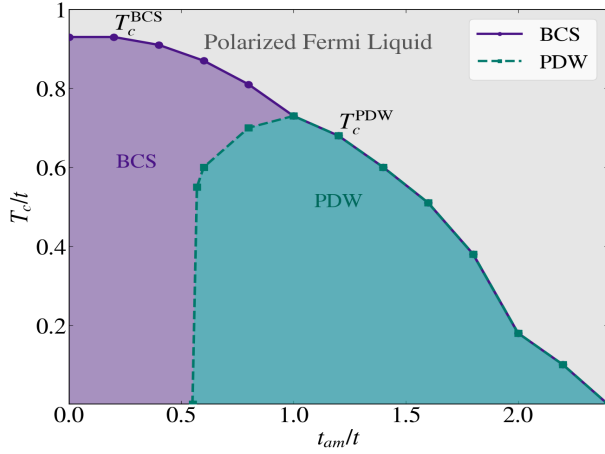


FIG. 7. Thermal phase diagram as obtained from the variational mean field theory, showing the BCS and PDW phases and the corresponding thermal scales T_c^{BCS} and T_c^{PDW} . Note that while the thermodynamic phases and the order of phase transitions are well captured by MFT, the thermal scales are overestimated.

variational parameters to optimize the energy. In the spirit of MFT we treat $|\Delta_{ij}| = |\Delta|$ as a real number and fix $\phi_{ij}^{rel} = \pi$. The trial periodic configurations for plausible SC phases are defined as, (i) $\Delta_{ij} \sim |\Delta| \cos(qx_i)$, (ii) $\Delta_{ij} \sim |\Delta|(\cos(qx_i) + \cos(qy_j))$ and (iii) $\Delta_{ij} \sim |\Delta| \cos q(x_i + y_i)$, corresponding to the uniaxial (1D), biaxial (2D) and diagonal modulated states, respectively. The ground state energy is optimized over the $t_{am} - h$ plane at a temperature of $T = 10^{-2}t$, for $U = -4t$, in the grand canonical ensemble with $\mu = -0.2t$ corresponding to a fermionic number density of $n \approx 0.9$.

The ground state ($T = 0.01t$) phase diagram in the $t_{am} - h$ plane as obtained via variational MFT is shown in Fig.5, typified in terms of the thermodynamic and spectroscopic signatures shown in Fig.6. The thermodynamic phases are classified in terms of the pairing field amplitude ($|\Delta|$), pairing momentum (\mathbf{q}) and magnetization (m) as: (i) uniform d -wave BCS ($|\Delta| \neq 0$, $\mathbf{q} = 0$, $m = 0$), (ii) PDW ($|\Delta| \neq 0$, $\mathbf{q} \neq 0$, $m = 0$), (iii) 1D-LO ($|\Delta| \neq 0$, $q_x = 0$, $q_y \neq 0$, $m \neq 0$), (iv) 2D-LO ($|\Delta| \neq 0$, $q_x \neq 0$, $q_y \neq 0$, $m \neq 0$) and (v) PFL ($|\Delta| = 0$, $\mathbf{q} = 0$, $m \neq 0$). At $t_{am} = 0$ the $0 < h \lesssim h_{c1}$ regime can further be sub-divided into a uniform d -wave (BCS) superconductor ($0 < h \lesssim h_{QBP}$) and a QBP phase ($h_{QBP} < h \lesssim h_{c1}$). The latter is a *gapless* SC phase quantified by $|\Delta| \neq 0$, $\mathbf{q} = 0$, $m \neq 0$ and characterized by a finite spectral weight at the Fermi level in the single particle DOS. It is a phase cohered, spatially inhomogeneous SC state with complementary magnetization in the form of spatially isolated islands without any periodicity and (quasi) long range correlations [16, 17]. Since this work focuses on the $\mathbf{q} \neq 0$ SC states in the $t_{am} - h - T$ space we didn't analyze the QBP phase in this manuscript and have referred to all the $\mathbf{q} = 0$ phases as BCS.

In Fig.6(a)-(c) we show the optimized $|\Delta|$, \mathbf{q} and m , respectively, across the $t_{am} - h$ cross sections. The $t_{am} = 0$

limit essentially corresponds to the d -wave BCS state, ALM ($t_{am} \neq 0$) weakly suppresses $|\Delta|$ (Fig.6(a)) and simultaneously promotes $\mathbf{q} \neq 0$ pairing (Fig.6(b)), leading to a SC state with collinear ($\mathbf{q} = \{0, \pi\}$) pairing momentum. In contrast to the conventional FFLO states the $\mathbf{q} \neq 0$ PDW state at $h = 0$, $t_{am} \neq 0$ is devoid of any magnetization, as observed from Fig.6(c). Based on the pairing field amplitude and momentum we define the critical ALM scales at the ground state as, (i) $t_{am}^c \sim 0.6t$ and (ii) $t_{am}^{sc} \sim 2.4t$, demarcating the second order transitions between BCS-PDW and PDW-PFL phases, respectively. In a similar spirit, the applied Zeeman field regime $0 < h \lesssim h_{c1} \sim 0.8t$ corresponds to the BCS state for $0 < t_{am} \lesssim t_{am}^c$ and to a 1D-LO phase for $t_{am}^c < t_{am} \lesssim t_{am}^{sc}$. The Zeeman field promotes FFLO pairing, such that, a first order transition takes place across h_{c1} and a non-collinear $\{q, q\}$ 2D-LO state sets in over the regime $h_{c1} < h \lesssim h_{c2}$. The LO phases via second order transition gives way to the PFL for $h \gtrsim h_{c2}$ and $t_{am} \gtrsim t_{am}^{sc}$.

The real space maps for the pairing field amplitude at the selected $t_{am} - h$ cross sections at the ground state are shown in Fig.6(d), while the corresponding spin resolved Fermi surface topology as determined from the low energy spectral weight distribution $A^\sigma(\mathbf{k}, 0)$ are presented in Fig.6(e) and Fig.6(f). ALM interactions lead to Fermi surface segmentation akin to the observation reported over a large class of SC systems such as, magnetic superconductor [151–155], magnet-superconductor hybrid [156–158], helical superconductor [159–164] etc. and arises due to the finite momentum scattering of the quasiparticles. Spatially modulated paired states at $t_{am} = 0.6t$ are shown for $h = 0.9t$ and $h = 1.2t$, representing the 1D- and 2D-LO phases, respectively. The Zeeman field induced imbalance in the population of the fermionic species ($m \neq 0$) is depicted in Fig.6(e) and Fig.6(f). We note that as compared to SPA the variational MFT calculations overestimates the stability of the PDW state even at the ground state with the MFT and SPA estimates of the critical parameters being $t_{am}^c \sim 0.6t$, $t_{am}^{sc} \sim 2.2t$ and $t_{am}^c \sim 0.8t$, $t_{am}^{sc} \sim 1.4t$, respectively. We have discussed the thermal phase diagram in the $t_{am} - T$ plane as obtained via SPA in the main text and shown that the thermal transition and crossover scales are captured with reasonable accuracy. The variational MFT grossly overestimates the thermal transition scales owing to its neglect of the fluctuations of the SC correlations. To establish the same we show the thermal phase diagram as obtained via the variational MFT in Fig.7. For $0 < t_{am} \lesssim t_{am}^c$ the uniform d -wave (BCS) SC state is realized which gives way to the PDW phase for $t_{am}^c < t_{am} \lesssim t_{am}^{sc}$. Thermal transitions to the PFL from both these phases are of second order.

FFLO vs PDW: We compare and contrast the finite temperature FFLO and PDW phases at $t_{am} = 1.0t$ and $T = 0.02t$ in terms of the pairing field amplitude ($|\Delta_{ij}|$) and magnetization (m_i) in Fig.8, at selected h/t values. At $t_{am} = 1.0t$ the ground state is PDW for $h = 0.0t$, characterized by uniaxial modulation in the pairing field amplitude and a net zero magnetization as shown in Fig.8. Zeeman field induces a finite magnetization due to imbalance in the population of the

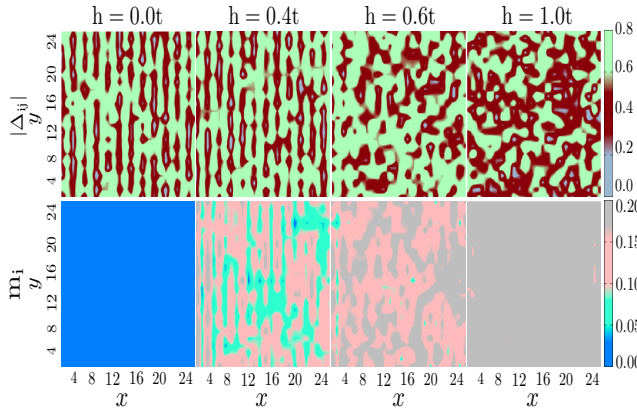


FIG. 8. Real space maps showing Zeeman field dependence of pairing field amplitude ($|\Delta_{ij}|$) and magnetization (m_i) at $t_{am} = 1.0t$ and $T = 0.02t$, highlighting the complementary behavior of the SC and magnetic correlations in the FFLO phase and the absence of magnetization in the PDW phase.

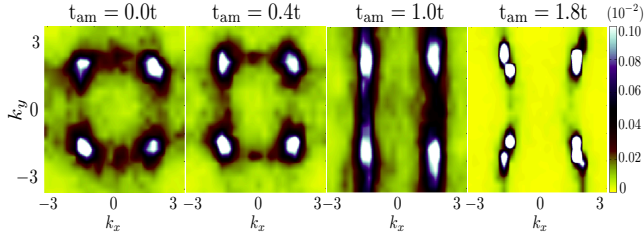


FIG. 9. Evolution of the Fermi surface at $T = 0.02t$ and $h = 0.0t$ in terms of the low energy spectral weight distribution ($A_{\uparrow}(\mathbf{k}, 0)$) as a function of the ALM interaction t_{am} , in the PDW phase. The $A_{\downarrow}(\mathbf{k}, 0)$ behaves identically. Note how the Fermi surface topology changes from the point nodes to the line nodes with t_{am} .

fermionic species. The SC state however undergoes disordering and spatial fragmentation with progressive increase in the Zeeman field. The strong Zeeman field regime of $h = 1.0t$ is typified by a large magnetization and a random SC phase with local SC correlations but no (quasi) long range coherence.

Fermi surface evolution: At a finite temperature of $T = 0.02t$ we show the low energy spectral weight distribution depicting the Fermi surface evolution at selected t_{am} across the d -wave BCS and PDW phases, in Fig.9. ALM doesn't create an imbalance in the fermionic population and therefore the Fermi surfaces corresponding to the \uparrow - and \downarrow -spin species are essentially degenerate. The nodal Fermi surface for $t_{am} < t_{am}^c$ typified by spectral weight accumulation at the point gap nodes depict the uniform d -wave SC pairing. In contrast the collinear PDW is characterized by line nodes [44]. For $t_{am} > t_{am}^{sc}$ the PDW correlations are lost and the d -wave symmetry of the Fermi surface (owing to $t_{am} \neq 0$) is observed.

At a representative ALM interaction of $t_{am} = 1.0t$ the evolution of the spin-resolved Fermi surface w. r. t. an applied Zeeman field is shown next in Fig.10. While the line nodes

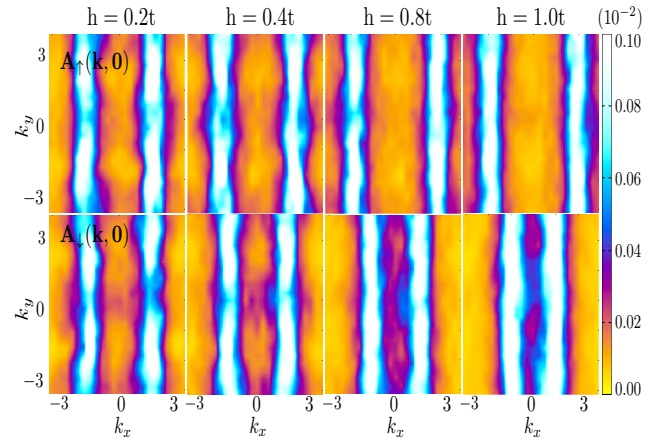


FIG. 10. Evolution of the spin-resolved Fermi surface in terms of the low energy spectral weight distribution $A_{\uparrow}(\mathbf{k}, 0)$ (upper panels) and $A_{\downarrow}(\mathbf{k}, 0)$ (lower panels) as a function of the Zeeman field, at $T = 0.02t$ and $t_{am} = 1.0t$. The spin-dependent mismatch in the Fermi surface depicts the imbalance in the population of the fermionic species.

are the clear signatures of ALM interaction, the applied Zeeman field results in Fermi surface mismatch which gets pronounced with increasing h/t .

* madhuparna.k@gmail.com

- [1] Peter Fulde and Richard A. Ferrell, "Superconductivity in a strong spin-exchange field," *Phys. Rev.* **135**, A550–A563 (1964).
- [2] A I Larkin and Yu N Ovchinnikov, "Nonuniform state of superconductors," *Zh. Eksp. Teor. Fiz.* **47**, 1136 (1964).
- [3] G. Sarma, "On the influence of a uniform exchange field acting on the spins of the conduction electrons in a superconductor," *Journal of Physics and Chemistry of Solids* **24**, 1029–1032 (1963).
- [4] Madhuparna Karmakar and Pinaki Majumdar, "Population-imbalanced lattice fermions near the bcs-bec crossover: Thermal physics of the breached pair and fulde-ferrell-larkin-ovchinnikov phases," *Phys. Rev. A* **93**, 053609 (2016).
- [5] Madhuparna Karmakar, "Thermal transitions, pseudogap behavior, and bcs-bec crossover in fermi-fermi mixtures," *Phys. Rev. A* **97**, 033617 (2018).
- [6] T. K. Koponen, T. Paananen, J.-P. Martikainen, and P. Törmä, "Finite-temperature phase diagram of a polarized fermi gas in an optical lattice," *Phys. Rev. Lett.* **99**, 120403 (2007).
- [7] P. G. De Gennes and G. Sarma, "Some Relations Between Superconducting and Magnetic Properties," *Journal of Applied Physics* **34**, 1380–1385 (1963).
- [8] W. Vincent Liu, Frank Wilczek, and Peter Zoller, "Spin-dependent hubbard model and a quantum phase transition in cold atoms," *Phys. Rev. A* **70**, 033603 (2004).
- [9] A. B. Vorontsov, J. A. Sauls, and M. J. Graf, "Phase diagram and spectroscopy of fulde-ferrell-larkin-ovchinnikov states of two-dimensional d -wave superconductors," *Phys. Rev. B* **72**, 184501 (2005).
- [10] Anton B. Vorontsov and Matthias J. Graf, "Fermi-liquid

- effects in the fulde-ferrell-larkin-ovchinnikov state of two-dimensional d -wave superconductors,” *Phys. Rev. B* **74**, 172504 (2006).
- [11] Jan Kaczmarczyk, Mariusz Sadzikowski, and Jozef Spałek, “Conductance spectroscopy of a correlated superconductor in a magnetic field in the pauli limit: Evidence for strong correlations,” *Phys. Rev. B* **84**, 094525 (2011).
- [12] Robert Beaird, Anton B. Vorontsov, and Ilya Vekhter, “Pauli-limited superconductivity with classical magnetic fluctuations,” *Phys. Rev. B* **81**, 224501 (2010).
- [13] Youichi Yanase, “Fflo superconductivity near the antiferromagnetic quantum critical point,” *Journal of the Physical Society of Japan* **77**, 063705 (2008).
- [14] Tao Zhou and C. S. Ting, “Phase diagram and local tunneling spectroscopy of the fulde-ferrell-larkin-ovchinnikov states of a two-dimensional square-lattice d -wave superconductor,” *Phys. Rev. B* **80**, 224515 (2009).
- [15] Qinghong Cui, C.-R. Hu, J. Y. T. Wei, and Kun Yang, “Spectroscopic signatures of the larkin-ovchinnikov state in the conductance characteristics of a normal-metal/superconductor junction,” *Phys. Rev. B* **85**, 014503 (2012).
- [16] Madhuparna Karmakar, “Pauli limited d -wave superconductors: quantum breached pair phase and thermal transitions,” *Journal of Physics: Condensed Matter* **32**, 405604 (2020).
- [17] Madhuparna Karmakar, “Magnetotransport and fermi surface segmentation in pauli limited superconductors,” *Journal of Physics: Condensed Matter* **36**, 165601 (2024).
- [18] A. Bianchi, R. Movshovich, C. Capan, P. G. Pagliuso, and J. L. Sarrao, “Possible fulde-ferrell-larkin-ovchinnikov superconducting state in cecoins₅,” *Phys. Rev. Lett.* **91**, 187004 (2003).
- [19] T. Tayama, A. Harita, T. Sakakibara, Y. Haga, H. Shishido, R. Settai, and Y. Onuki, “Unconventional heavy-fermion superconductor cecoins₅: dc magnetization study at temperatures down to 50 mk,” *Phys. Rev. B* **65**, 180504 (2002).
- [20] G. Koutroulakis, M. D. Stewart, V. F. Mitrović, M. Horvatić, C. Berthier, G. Lapertot, and J. Flouquet, “Field evolution of coexisting superconducting and magnetic orders in cecoins₅,” *Phys. Rev. Lett.* **104**, 087001 (2010).
- [21] M. Kenzelmann, Th. Strässle, C. Niedermayer, M. Sigrist, B. Padmanabhan, M. Zolliker, A. D. Bianchi, R. Movshovich, E. D. Bauer, J. L. Sarrao, and J. D. Thompson, “Coupled superconducting and magnetic order in cecoins₅,” *Science* **321**, 1652 (2008).
- [22] C. Capan, A. Bianchi, R. Movshovich, A. D. Christianson, A. Malinowski, M. F. Hundley, A. Lacerda, P. G. Pagliuso, and J. L. Sarrao, “Anisotropy of thermal conductivity and possible signature of the fulde-ferrell-larkin-ovchinnikov state in CeCoin₅,” *Phys. Rev. B* **70**, 134513 (2004).
- [23] C. Martin, C. C. Agosta, S. W. Tozer, H. A. Radovan, E. C. Palm, T. P. Murphy, and J. L. Sarrao, “Evidence for the fulde-ferrell-larkin-ovchinnikov state in cecoins₅ from penetration depth measurements,” *Phys. Rev. B* **71**, 020503 (2005).
- [24] Simon Gerber, Marek Bartkowiak, Jorge L. Gavilano, Eric Ressouche, Nikola Egetenmeyer, Christof Niedermayer, Andrea D. Bianchi, Roman Movshovich, Eric D. Bauer, Joe D. Thompson, and Michel Kenzelmann, “Switching of magnetic domains reveals spatially inhomogeneous superconductivity,” *Nature Physics* **10**, 126 (2014).
- [25] K. Kumagai, M. Saitoh, T. Oyaizu, Y. Furukawa, S. Takashima, M. Nohara, H. Takagi, and Y. Matsuda, “Fulde-ferrell-larkin-ovchinnikov state in a perpendicular field of quasi-two-dimensional cecoins₅,” *Phys. Rev. Lett.* **97**, 227002 (2006).
- [26] Duk Y. Kim, Shi-Zeng Lin, Franziska Weickert, Michel Kenzelmann, Eric D. Bauer, Filip Ronning, J. D. Thompson, and Roman Movshovich, “Intertwined orders in heavy-fermion superconductor cecoins₅,” *Phys. Rev. X* **6**, 041059 (2016).
- [27] Shi-Zeng Lin, Duk Y. Kim, Eric D. Bauer, Filip Ronning, J. D. Thompson, and Roman Movshovich, “Interplay of the spin density wave and a possible fulde-ferrell-larkin-ovchinnikov state in cecoins₅ in rotating magnetic field,” *Phys. Rev. Lett.* **124**, 217001 (2020).
- [28] R. Beyer and J. Wosnitza, “Emerging evidence for fflo states in layered organic superconductors,” *Low Temperature Physics* **39**, 225–231 (2013).
- [29] R. Lortz, Y. Wang, A. Demuer, P. H. M. Böttger, B. Bergk, G. Zwicknagl, Y. Nakazawa, and J. Wosnitza, “Calorimetric evidence for a fulde-ferrell-larkin-ovchinnikov superconducting state in the layered organic superconductor κ -(BEDT-TTF)₂Cu(NCS)₂,” *Phys. Rev. Lett.* **99**, 187002 (2007).
- [30] H. Mayaffre, S. Krämer, M. Horvatić, C. Berthier, K. Miyagawa, K. Kanoda, and V. F. Mitrović, “Evidence of andreev bound states as a hallmark of the fflo phase in κ -(bedt-ttf)₂cu(ncs)₂,” *Nature Physics* **10**, 928 (2014).
- [31] J. A. Wright, E. Green, P. Kuhns, A. Reyes, J. Brooks, J. Schlueter, R. Kato, H. Yamamoto, M. Kobayashi, and S. E. Brown, “Zeeman-driven phase transition within the superconducting state of κ -(BEDT-TTF)₂Cu(NCS)₂,” *Phys. Rev. Lett.* **107**, 087002 (2011).
- [32] William A. Coniglio, Laurel E. Winter, Kyuil Cho, C. C. Agosta, B. Fravel, and L. K. Montgomery, “Superconducting phase diagram and fflo signature in λ -(bets)₂gacl₄ from rf penetration depth measurements,” *Phys. Rev. B* **83**, 224507 (2011).
- [33] B. Bergk, A. Demuer, I. Sheikin, Y. Wang, J. Wosnitza, Y. Nakazawa, and R. Lortz, “Magnetic torque evidence for the fulde-ferrell-larkin-ovchinnikov state in the layered organic superconductor κ -(BEDT-TTF)₂Cu(NCS)₂,” *Phys. Rev. B* **83**, 064506 (2011).
- [34] C. C. Agosta, Jing Jin, W. A. Coniglio, B. E. Smith, K. Cho, I. Stroe, C. Martin, S. W. Tozer, T. P. Murphy, E. C. Palm, J. A. Schlueter, and M. Kurmoo, “Experimental and semiempirical method to determine the pauli-limiting field in quasi-two-dimensional superconductors as applied to κ -(bedt-ttf)₂cu(ncs)₂: Strong evidence of a fflo state,” *Phys. Rev. B* **85**, 214514 (2012).
- [35] K. Cho, B. E. Smith, W. A. Coniglio, L. E. Winter, C. C. Agosta, and J. A. Schlueter, “Upper critical field in the organic superconductor β ''-(ET)₂Sf₅Ch₂F₂SO₃: Possibility of fulde-ferrell-larkin-ovchinnikov state,” *Phys. Rev. B* **79**, 220507 (2009).
- [36] D. A. Zocco, K. Grube, F. Eilers, T. Wolf, and H. v. Löhneysen, “Pauli-limited multiband superconductivity in kfe₂as₂,” *Phys. Rev. Lett.* **111**, 057007 (2013).
- [37] K. Cho, H. Kim, M. A. Tanatar, Y. J. Song, Y. S. Kwon, W. A. Coniglio, C. C. Agosta, A. Gurevich, and R. Prozorov, “Anisotropic upper critical field and possible fulde-ferrell-larkin-ovchinnikov state in the stoichiometric pnictide superconductor lifeas,” *Phys. Rev. B* **83**, 060502 (2011).
- [38] Seunghyun Kim, Bumsung Lee, Jae Wook Kim, Eun Sang Choi, G. R. Stewart, and Kee Hoon Kim, “Pauli-limiting effects in the upper critical fields of a clean lifeas single crystal,” *Phys. Rev. B* **84**, 104502 (2011).
- [39] Yong-il Shin, Christian H. Schunck, André Schirotzek, and Wolfgang Ketterle, “Phase diagram of a two-component fermi gas with resonant interactions,” *Nature* **451**, 689 (2008).

- [40] C. H. Schunck, Y. Shin, A. Schirotzek, M. W. Zwierlein, and W. Ketterle, "Pairing without superfluidity: The ground state of an imbalanced fermi mixture," *Science* **316**, 867–870 (2007).
- [41] Y. Shin, M. W. Zwierlein, C. H. Schunck, A. Schirotzek, and W. Ketterle, "Observation of phase separation in a strongly interacting imbalanced fermi gas," *Phys. Rev. Lett.* **97**, 030401 (2006).
- [42] Yean-an Liao, Ann Sophie C. Rittner, Tobias Paprotta, Wenhui Li, Guthrie B. Partridge, Randall G. Hulet, Stefan K. Baur, and Erich J. Mueller, "Spin-imbalance in a one-dimensional fermi gas," *Nature* **467**, 567 (2010).
- [43] Shou cheng Zhang, "Recent developments in the so(5) theory of high T_c superconductivity," *Journal of Physics and Chemistry of Solids* **59**, 1774–1779 (1998).
- [44] Daniel F. Agterberg, J.C. Séamus Davis, Stephen D. Edkins, Eduardo Fradkin, Dale J. Van Harlingen, Steven A. Kivelson, Patrick A. Lee, Leo Radzihovsky, John M. Tranquada, and Yuxuan Wang, "The physics of pair-density waves: Cuprate superconductors and beyond," *Annual Review of Condensed Matter Physics* **11**, 231–270 (2020).
- [45] Erez Berg, Eduardo Fradkin, Steven A Kivelson, and John M Tranquada, "Striped superconductors: how spin, charge and superconducting orders intertwine in the cuprates," *New Journal of Physics* **11**, 115004 (2009).
- [46] Erez Berg, Eduardo Fradkin, and Steven A. Kivelson, "Pair-density-wave correlations in the kondo-heisenberg model," *Phys. Rev. Lett.* **105**, 146403 (2010).
- [47] Tilman Schwemmer, Hendrik Hohmann, Matteo Dürrnagel, Janik Potten, Jacob Beyer, Stephan Rachel, Yi-Ming Wu, Srinivas Raghu, Tobias Müller, Werner Hanke, and Ronny Thomale, "Sublattice modulated superconductivity in the kagome hubbard model," *Phys. Rev. B* **110**, 024501 (2024).
- [48] D. F. Agterberg and H. Tsunetsugu, "Dislocations and vortices in pair-density-wave superconductors," *Nature Physics* **4**, 639 (2008).
- [49] Erez Berg, Eduardo Fradkin, and Steven A. Kivelson, "Charge-4e superconductivity from pair-density-wave order in certain high-temperature superconductors," *Nature Physics* **5**, 830 (2009).
- [50] Eduardo Fradkin, Steven A. Kivelson, and John M. Tranquada, "Colloquium: Theory of intertwined orders in high temperature superconductors," *Rev. Mod. Phys.* **87**, 457–482 (2015).
- [51] Florian Loder, Arno P. Kampf, and Thilo Kopp, "Superconducting state with a finite-momentum pairing mechanism in zero external magnetic field," *Phys. Rev. B* **81**, 020511 (2010).
- [52] Yu-Xiao Jiang, Jia-Xin Yin, M. Michael Denner, Nana Shumiya, Brenden R. Ortiz, Gang Xu, Zurab Guguchia, Junyi He, Md Shafayat Hossain, Xiaoxiong Liu, Jacob Ruff, Linus Kautzsch, Songtian S. Zhang, Guoqing Chang, Ilya Belopolski, Qi Zhang, Tyler A. Cochran, Daniel Multer, Maksim Litskevich, Zi-Jia Cheng, Xian P. Yang, Ziqiang Wang, Ronny Thomale, Titus Neupert, Stephen D. Wilson, and M. Zahid Hasan, "Unconventional chiral charge order in kagome superconductor kv3sb5 ," *Nature Materials* **20**, 1353 (2021).
- [53] Hui Chen, Haitao Yang, Bin Hu, Zhen Zhao, Jie Yuan, Yuqing Xing, Guojian Qian, Zihao Huang, Geng Li, Yuhan Ye, Sheng Ma, Shunli Ni, Hua Zhang, Qiangwei Yin, Chunsheng Gong, Zhijun Tu, Hechang Lei, Hengxin Tan, Sen Zhou, Chengmin Shen, Xiaoli Dong, Binghai Yan, Ziqiang Wang, and Hong-Jun Gao, "Roton pair density wave in a strong-coupling kagome superconductor," *Nature* **599**, 222 (2021).
- [54] Qiangqiang Gu, Joseph P. Carroll, Shuqiu Wang, Sheng Ran, Christopher Broyles, Hasan Siddiquee, Nicholas P. Butch, Shanta R. Saha, Johnpierre Paglione, J. C. Séamus Davis, and Xiaolong Liu, "Detection of a pair density wave state in ute_2 ," *Nature* **618**, 921 (2023).
- [55] Anuva Aishwarya, Julian May-Mann, Arjun Raghavan, Laimei Nie, Marisa Romanelli, Sheng Ran, Shanta R. Saha, Johnpierre Paglione, Nicholas P. Butch, Eduardo Fradkin, and Vidya Madhavan, "Magnetic-field-sensitive charge density waves in the superconductor ute_2 ," *Nature* **618**, 928 (2023).
- [56] He Zhao, Raymond Blackwell, Morgan Thinel, Taketo Handa, Shigeyuki Ishida, Xiaoyang Zhu, Akira Iyo, Hiroshi Eisaki, Abhay N. Pasupathy, and Kazuhiro Fujita, "Smectic pair-density-wave order in eurf_4as_4 ," *Nature* **618**, 940 (2023).
- [57] Libor Šmejkal, Jairo Sinova, and Tomas Jungwirth, "Beyond conventional ferromagnetism and antiferromagnetism: A phase with nonrelativistic spin and crystal rotation symmetry," *Phys. Rev. X* **12**, 031042 (2022).
- [58] Cheng Song, Hua Bai, Zhiyuan Zhou, Lei Han, Helena Reichlova, J. Hugo Dil, Junwei Liu, Xianzhe Chen, and Feng Pan, "Altermagnets as a new class of functional materials," *Nature Reviews Materials* **10**, 473 (2025).
- [59] Soho Shim, M. Mehraeen, Joseph Sklenar, Steven S.-L. Zhang, Axel Hoffmann, and Nadya Mason, "Spin-polarized antiferromagnetic metals," *Annual Review of Condensed Matter Physics* **16**, 103 (2025).
- [60] Rafael M. Fernandes, Vanuilo S. de Carvalho, Turan Birol, and Rodrigo G. Pereira, "Topological transition from nodal to nodeless zeeman splitting in altermagnets," *Phys. Rev. B* **109**, 024404 (2024).
- [61] Igor I. Mazin, Klaus Koepf, Michelle D. Johannes, Rafael González-Hernández, and Libor Šmejkal, "Prediction of unconventional magnetism in doped $\text{fesb}_2\text{sub}_2\text{i}/\text{sub}_2\text{e}$," *Proceedings of the National Academy of Sciences* **118**, e2108924118 (2021).
- [62] "Spin-split collinear antiferromagnets: A large-scale ab-initio study," *Materials Today Physics* **32**, 100991 (2023).
- [63] Ze-Feng Gao, Shuai Qu, Bocheng Zeng, Yang Liu, Ji-Rong Wen, Hao Sun, Peng-Jie Guo, and Zhong-Yi Lu, "Ai-accelerated discovery of altermagnetic materials," *National Science Review* **12**, nwaf066 (2025).
- [64] Igor Mazin, Rafael González-Hernández, and Libor Šmejkal, "Induced monolayer altermagnetism in $\text{mnp}(\text{s},\text{se})_3$ and fese ," (2023), arXiv:2309.02355 [cond-mat.mes-hall].
- [65] Rodrigo Jaeschke-Ubiergo, Venkata Krishna Bharadwaj, Tomas Jungwirth, Libor Šmejkal, and Jairo Sinova, "Supercell altermagnets," *Phys. Rev. B* **109**, 094425 (2024).
- [66] Xuhao Wan, Subhasish Mandal, Yuzheng Guo, and Kristjan Haule, "High-throughput search for metallic altermagnets by embedded dynamical mean field theory," *Phys. Rev. Lett.* **135**, 106501 (2025).
- [67] Joachim Sødequist and Thomas Olsen, "Two-dimensional altermagnets from high throughput computational screening: Symmetry requirements, chiral magnons, and spin-orbit effects," *Applied Physics Letters* **124**, 182409.
- [68] Andriy Smolyanyuk, Libor Šmejkal, and Igor I. Mazin, "A tool to check whether a symmetry-compensated collinear magnetic material is antiferro- or altermagnetic," (2024), arXiv:2401.08784 [cond-mat.mtrl-sci].
- [69] Yixuan Che, Haifeng Lv, Xiaojun Wu, and Jinlong Yang, "Realizing altermagnetism in two-dimensional metal-organic framework semiconductors with electric-field-controlled anisotropic spin current," *Chem. Sci.* **15**, 10.1039/D4SC04125A.

- [70] Yixuan Che, Haifeng Lv, Xiaojun Wu, and Jinlong Yang, “Bi-layer metal–organic framework altermagnets with electrically tunable spin-split valleys,” *Journal of the American Chemical Society* **147**, 14806 (2025).
- [71] Romakanta Bhattarai, Peter Minch, and Trevor David Rhone, “High-throughput screening of altermagnetic materials,” *Phys. Rev. Mater.* **9**, 064403 (2025).
- [72] Mingqiang Gu, Yuntian Liu, Haiyuan Zhu, Kunihiro Yananose, Xiaobing Chen, Yongkang Hu, Alessandro Stroppa, and Qihang Liu, “Ferroelectric switchable altermagnetism,” *Phys. Rev. Lett.* **134**, 106802 (2025).
- [73] Xunkai Duan, Jiayong Zhang, Ziye Zhu, Yuntian Liu, Zhenyu Zhang, Igor Žutić, and Tong Zhou, “Antiferroelectric altermagnets: Antiferroelectricity alters magnets,” *Phys. Rev. Lett.* **134**, 106801 (2025).
- [74] Libor Šmejkal, “Altermagnetic multiferroics and altermagnetolectric effect,” (2024), [arXiv:2411.19928 \[cond-mat.mtrl-sci\]](https://arxiv.org/abs/2411.19928).
- [75] Cong Li, Mengli Hu, Zhilin Li, Yang Wang, Wanyu Chen, Balasubramanian Thiagarajan, Mats Leandersson, Craig Polley, Timur Kim, Hui Liu, Cosma Fulga, Maia G. Vergniory, Oleg Janson, Oscar Tjernberg, and Jeroen van den Brink, “Topological weyl altermagnetism in crsb,” *Communications Physics* **8**, 311 (2025).
- [76] Jianyang Ding, Zhicheng Jiang, Xiuhua Chen, Zicheng Tao, Zhengtai Liu, Tongrui Li, Jishan Liu, Jianping Sun, Jinguang Cheng, Jiayu Liu, Yichen Yang, Runfeng Zhang, Liwei Deng, Wenchuan Jing, Yu Huang, Yuming Shi, Mao Ye, Shan Qiao, Yilin Wang, Yanfeng Guo, Donglai Feng, and Dawei Shen, “Large band splitting in g-wave altermagnet crsb,” *Phys. Rev. Lett.* **133**, 206401 (2024).
- [77] Guowei Yang, Zhanghuan Li, Sai Yang, Jiyuan Li, Hao Zheng, Weifan Zhu, Ze Pan, Yifu Xu, Saizheng Cao, Wenxuan Zhao, Anupam Jana, Jiawen Zhang, Mao Ye, Yu Song, Lun-Hui Hu, Lexian Yang, Jun Fujii, Ivana Vobornik, Ming Shi, Huiqiu Yuan, Yongjun Zhang, Yuanfeng Xu, and Yang Liu, “Three-dimensional mapping of the altermagnetic spin splitting in crsb,” *Nature Communications* **16**, 1442 (2025).
- [78] Wenlong Lu, Shiyu Feng, Yuzhi Wang, Dong Chen, Zihan Lin, Xin Liang, Siyuan Liu, Wanxiang Feng, Kohei Yamagami, Junwei Liu, Claudia Felser, Quansheng Wu, and Junzhang Ma, “Signature of topological surface bands in altermagnetic weyl semimetal crsb,” *Nano Letters* **25**, 7343 (2025).
- [79] Bei Jiang, Mingzhe Hu, Jianli Bai, Ziyin Song, Chao Mu, Gexing Qu, Wan Li, Wenliang Zhu, Hanqi Pi, Zhongxu Wei, Yu-Jie Sun, Yaobo Huang, Xiquan Zheng, Yingying Peng, Lunhua He, Shiliang Li, Jianlin Luo, Zheng Li, Genfu Chen, Hang Li, Hongming Weng, and Tian Qian, “A metallic room-temperature d-wave altermagnet,” *Nature Physics* **21**, 754 (2025).
- [80] Fayuan Zhang, Xingkai Cheng, Zhouyi Yin, Changchao Liu, Liwei Deng, Yuxi Qiao, Zheng Shi, Shuxuan Zhang, Junhao Lin, Zhengtai Liu, Mao Ye, Yaobo Huang, Xiangyu Meng, Cheng Zhang, Taichi Okuda, Kenya Shimada, Shengtao Cui, Yue Zhao, Guang-Han Cao, Shan Qiao, Junwei Liu, and Chaoyu Chen, “Crystal-symmetry-paired spin–valley locking in a layered room-temperature metallic altermagnet candidate,” *Nature Physics* **21**, 760 (2025).
- [81] I. I. Mazin, “Altermagnetism in mnte: Origin, predicted manifestations, and routes to detwinning,” *Phys. Rev. B* **107**, L100418 (2023).
- [82] Suyoung Lee, Sangjae Lee, Saegyeol Jung, Jiwon Jung, Donghan Kim, Yeonjae Lee, Byeongjun Seok, Jaeyoung Kim, Byeong Gyu Park, Libor Šmejkal, Chang-Jong Kang, and Changyoung Kim, “Broken kramers degeneracy in altermagnetic mnte,” *Phys. Rev. Lett.* **132**, 036702 (2024).
- [83] T. Osumi, S. Souma, T. Aoyama, K. Yamauchi, A. Honma, K. Nakayama, T. Takahashi, K. Ohgushi, and T. Sato, “Observation of a giant band splitting in altermagnetic mnte,” *Phys. Rev. B* **109**, 115102 (2024).
- [84] J. Krempaský, L. Šmejkal, S. W. D’Souza, M. Hajlaoui, G. Springholz, K. Uhlířová, F. Alarab, P. C. Constantinou, V. Strocov, D. Usanov, W. R. Pudelko, R. González-Hernández, A. Birk Hellenes, Z. Jansa, H. Reichlová, Z. Šobáň, R. D. Gonzalez Betancourt, P. Wadley, J. Sinova, D. Kriegner, J. Minár, J. H. Dil, and T. Jungwirth, “Altermagnetic lifting of kramers spin degeneracy,” *Nature* **626**, 517 (2024).
- [85] Chao-Chun Wei, Xiaoyin Li, Sabrina Hatt, Xudong Huai, Jue Liu, Birender Singh, Kyung-Mo Kim, Rafael M. Fernandes, Paul Cardon, Liuyan Zhao, Thao T. Tran, Benjamin A. Frandsen, Kenneth S. Burch, Feng Liu, and Huiwen Ji, “ $\text{Ia}_2\text{O}_3\text{Mn}_2\text{Se}_2$: A correlated insulating layered d-wave altermagnet,” *Phys. Rev. Mater.* **9**, 024402 (2025).
- [86] Laura Garcia-Gassull, Aleksandar Razpopov, Panagiotis Peter Stavropoulos, Igor I Mazin, and Roser Valentí, “Microscopic origin of the magnetic interactions and their experimental signatures in altermagnetic $\text{Ia}_2\text{O}_3\text{Mn}_2\text{Se}_2$,” (2025), [arXiv:2506.21661 \[cond-mat.str-el\]](https://arxiv.org/abs/2506.21661).
- [87] Satoshi Iguchi, Hiroki Kobayashi, Yuka Ikemoto, Tetsuya Furukawa, Hirotake Itoh, Shinichiro Iwai, Taro Moriwaki, and Takahiko Sasaki, “Magneto-optical spectra of an organic antiferromagnet as a candidate for an altermagnet,” *Phys. Rev. Res.* **7**, 033026 (2025).
- [88] Fabio Bernardini, Manfred Fiebig, and Andrés Cano, “Ruddlesden–popper and perovskite phases as a material platform for altermagnetism,” *Journal of Applied Physics* **137**, 103903 (2025).
- [89] Makoto Naka, Yukitoshi Motome, and Hitoshi Seo, “Altermagnetic perovskites,” *npj Spintronics* **3**, 1 (2025).
- [90] Francesco Ferrari and Roser Valentí, “Altermagnetism on the shastry–sutherland lattice,” *Phys. Rev. B* **110**, 205140 (2024).
- [91] João Augusto Sobral, Subrata Mandal, and Mathias S. Scheurer, “Fractionalized altermagnets: From neighboring and altermagnetic spin liquids to spin-symmetric band splitting,” *Phys. Rev. Res.* **7**, 023152 (2025).
- [92] Samuele Giuli, Carlos Mejuto-Zaera, and Massimo Capone, “Altermagnetism from interaction-driven itinerant magnetism,” *Phys. Rev. B* **111**, L020401 (2025).
- [93] Zhenfeng Ouyang, Peng-Jie Guo, Rong-Qiang He, and Zhong-Yi Lu, “Strongly correlated altermagnet CaCrO_3 ,” (2025), [arXiv:2507.14081 \[cond-mat.str-el\]](https://arxiv.org/abs/2507.14081).
- [94] Tomas Jungwirth, Jairo Sinova, Rafael M. Fernandes, Qihang Liu, Hikaru Watanabe, Shuichi Murakami, Satoru Nakatsuji, and Libor Šmejkal, “Symmetry, microscopy and spectroscopy signatures of altermagnetism,” (2025), [arXiv:2506.22860 \[cond-mat.mtrl-sci\]](https://arxiv.org/abs/2506.22860).
- [95] Ina Park, Turan Birol, Antoine Georges, and Rafael M. Fernandes, “Impact of strong electronic correlations on altermagnets: the case of NiS_2 ,” (2025), [arXiv:2512.17059 \[cond-mat.str-el\]](https://arxiv.org/abs/2512.17059).
- [96] Nitin Kaushal and Marcel Franz, “Altermagnetism in modified lieb lattice hubbard model,” *Phys. Rev. Lett.* **135**, 156502 (2025).
- [97] Matteo Dürrnagel, Hendrik Hohmann, Atanu Maity, Jannis Seufert, Michael Klett, Lennart Klebl, and Ronny Thomale, “Altermagnetic phase transition in a lieb metal,” *Phys. Rev. Lett.* **135**, 036502 (2025).

- [98] Wenjun Zhao, Yuri Fukaya, Pablo Buset, Jorge Cayao, Yukio Tanaka, and Bo Lu, "Orientation-dependent transport in junctions formed by d -wave altermagnets and d -wave superconductors," *Phys. Rev. B* **111**, 184515 (2025).
- [99] Bo Lu, Phillip Mercebach, Pablo Buset, Keiji Yada, Jorge Cayao, Yukio Tanaka, and Yuri Fukaya, "Engineering sub-gap states in superconductors by the symmetry of altermagnetism," (2026), [arXiv:2508.03364 \[cond-mat.supr-con\]](https://arxiv.org/abs/2508.03364).
- [100] Yuri Fukaya, Bo Lu, Keiji Yada, Yukio Tanaka, and Jorge Cayao, "Crossed surface flat bands in three-dimensional superconducting altermagnets," *Phys. Rev. Lett.* (2026), [10.1103/65q6-5wxl](https://arxiv.org/abs/2510.1103).
- [101] Yuri Fukaya, Keiji Yada, and Yukio Tanaka, " p -wave superconductivity and josephson current in p -wave unconventional magnet/ s -wave superconductor hybrid systems," (2026), [arXiv:2512.18636 \[cond-mat.supr-con\]](https://arxiv.org/abs/2512.18636).
- [102] Bo Lu, Kazuki Maeda, Hiroyuki Ito, Keiji Yada, and Yukio Tanaka, " φ josephson junction induced by altermagnetism," *Phys. Rev. Lett.* **133**, 226002 (2024).
- [103] Kazuki Maeda, Yuri Fukaya, Keiji Yada, Bo Lu, Yukio Tanaka, and Jorge Cayao, "Classification of pair symmetries in superconductors with unconventional magnetism," *Phys. Rev. B* **111**, 144508 (2025).
- [104] Kazuki Maeda, Bo Lu, Keiji Yada, and Yukio Tanaka, "Theory of tunneling spectroscopy in unconventional p -wave magnet-superconductor hybrid structures," *Journal of the Physical Society of Japan* **93**, 114703 (2024).
- [105] Yuri Fukaya, Bo Lu, Keiji Yada, Yukio Tanaka, and Jorge Cayao, "Superconducting phenomena in systems with unconventional magnets," *Journal of Physics: Condensed Matter* **37**, 313003 (2025).
- [106] Shuntaro Sumita, Makoto Naka, and Hitoshi Seo, "Phase-modulated superconductivity via altermagnetism," *Phys. Rev. B* **112**, 144510 (2025).
- [107] Song-Bo Zhang, Lun-Hui Hu, and Titus Neupert, "Finite-momentum cooper pairing in proximitized altermagnets," *Nature Communications* **15**, 1801 (2024).
- [108] Hui Hu, Zhao Liu, Jia Wang, Xia-Ji Liu, and Yoji Ohashi, "Finite-momentum superconductivity with singlet-triplet mixing in an altermagnetic metal: A pairing instability analysis," (2026), [arXiv:2603.12897 \[cond-mat.supr-con\]](https://arxiv.org/abs/2603.12897).
- [109] GiBaik Sim and Johannes Knolle, "Pair density waves and supercurrent diode effect in altermagnets," *Phys. Rev. B* **112**, L020502 (2025).
- [110] Debmalya Chakraborty and Annica M. Black-Schaffer, "Zero-field finite-momentum and field-induced superconductivity in altermagnets," *Phys. Rev. B* **110**, L060508 (2024).
- [111] Debmalya Chakraborty and Annica M. Black-Schaffer, "Perfect superconducting diode effect in altermagnets," *Phys. Rev. Lett.* **135**, 026001 (2025).
- [112] Anjishnu Bose, Samuel Vadnais, and Arun Paramakanti, "Altermagnetism and superconductivity in a multiorbital $t - j$ model," *Phys. Rev. B* **110**, 205120 (2024).
- [113] Xuan Zou, Rafael M. Fernandes, and Eduardo Fradkin, "Superconducting states and intertwined orders in metallic altermagnets," (2026), [arXiv:2603.04503 \[cond-mat.supr-con\]](https://arxiv.org/abs/2603.04503).
- [114] Kinga Jasiewicz, Paweł Wójcik, Michał P. Nowak, and Michał Zegrodnik, "Interplay between altermagnetism and superconductivity in two dimensions: intertwined symmetries and singlet-triplet mixing," *npj Quantum Materials* (2025), [10.1038/s41535-025-00840-w](https://arxiv.org/abs/2510.1038).
- [115] SeungBeom Hong, Moon Jip Park, and Kyoung-Min Kim, "Unconventional p -wave and finite-momentum superconductivity induced by altermagnetism through the formation of bogoliubov fermi surface," *Phys. Rev. B* **111**, 054501 (2025).
- [116] Miaomiao Wei, Longjun Xiang, Fuming Xu, Lei Zhang, Gaomin Tang, and Jian Wang, "Gapless superconducting state and mirage gap in altermagnets," *Phys. Rev. B* **109**, L201404 (2024).
- [117] Jabir Ali Ouassou, Arne Brataas, and Jacob Linder, "dc josephson effect in altermagnets," *Phys. Rev. Lett.* **131**, 076003 (2023).
- [118] Michał Papaj, "Andreev reflection at the altermagnet-superconductor interface," *Phys. Rev. B* **108**, L060508 (2023).
- [119] J. Hubbard, "Calculation of partition functions," *Phys. Rev. Lett.* **3**, 77–78 (1959).
- [120] H. J. Schulz, "Effective action for strongly correlated fermions from functional integrals," *Phys. Rev. Lett.* **65**, 2462–2465 (1990).
- [121] Simone Fratini and Sergio Ciuchi, "Displaced drude peak and bad metal from the interaction with slow fluctuations," *SciPost Phys.* **11**, 039 (2021).
- [122] Sergio Ciuchi and Simone Fratini, "Strange metal behavior from incoherent carriers scattered by local moments," *Phys. Rev. B* **108**, 235173 (2023).
- [123] Chaitanya Murthy, Akshat Pandey, Ilya Esterlis, and Steven A. Kivelson, "A stability bound on the t -linear resistivity of conventional metals," *Proceedings of the National Academy of Sciences* **120**, e2216241120 (2023).
- [124] Shashikant Singh Kunwar and Madhuparna Karmakar, "Straintronics across lieb-kagome interconversion and variable transport scaling exponents," *Phys. Rev. Mater.* **10**, L011002 (2026).
- [125] Yuanzhe Li, Yilin Han, Liu Yang, Wanli He, Pengda Ye, Wencheng Huang, Jiabin Qiao, Yuemei Li, Xiaodong Sun, Tingli He, Jiayi Han, Yuxiang Chen, Ruifeng Tian, Hao Sun, Yuwei Liu, Feng Wu, Baoshan Song, Zhengtai Liu, Mao Ye, Yaobo Huang, Kenichi Ozawa, Ji Dai, Massimo Talarida, Shengtao Cui, Jie Chen, Meiling Jin, Wayne Zheng, Chaoyu Chen, Zhiwei Wang, Zhi-Ming Yu, Xiang Li, and Yugui Yao, "Pressure-induced superconducting-like transition in the d -wave altermagnet candidate $\text{CsV}_2\text{Se}_2\text{O}_8$," (2026), [arXiv:2604.09457 \[cond-mat.supr-con\]](https://arxiv.org/abs/2604.09457).
- [126] Shirir Baruch and Dror Orgad, "Spectral signatures of modulated d -wave superconducting phases," *Phys. Rev. B* **77**, 174502 (2008).
- [127] Ken Matsuba, Shunsuke Yoshizawa, Yugo Mochizuki, Takashi Mochiku, Kazuto Hirata, and Nobuhiko Nishida, "Anti-phase modulation of electron- and hole-like states in vortex core of $\text{Bi}_2\text{Sr}_2\text{CaCu}_2\text{O}_x$ probed by scanning tunneling spectroscopy," *Journal of the Physical Society of Japan* **76**, 063704 (2007).
- [128] Shunsuke Yoshizawa, Taiji Koseki, Ken Matsuba, Takashi Mochiku, Kazuto Hirata, and Nobuhiko Nishida, "High-resolution scanning tunneling spectroscopy of vortex cores in inhomogeneous electronic states of $\text{Bi}_2\text{Sr}_2\text{CaCu}_2\text{O}_x$," *Journal of the Physical Society of Japan* **82**, 083706 (2013).
- [129] T. Machida, Y. Kohsaka, K. Matsuoka, K. Iwaya, T. Hanaguri, and T. Tamegai, "Bipartite electronic superstructures in the vortex core of $\text{Bi}_2\text{Sr}_2\text{CaCu}_2\text{O}_{8+\delta}$," *Nature Communications* **7**, 2041 (2016).
- [130] S. D. Edkins, A. Kostin, K. Fujita, A. P. Mackenzie, H. Eisaki, S. Uchida, Subir Sachdev, Michael J. Lawler, E.-A. Kim, J. C. Séamus Davis, and M. H. Hamidian, "Magnetic field-induced pair density wave state in the cuprate vortex halo," *Science* **364**, 976–980 (2019).
- [131] Y. Kohsaka, C. Taylor, K. Fujita, A. Schmidt, C. Lupien, T. Hanaguri, M. Azuma, M. Takano, H. Eisaki, H. Takagi,

- S. Uchida, and J. C. Davis, “An intrinsic bond-centered electronic glass with unidirectional domains in underdoped cuprates,” *Science* **315**, 1380–1385 (2007).
- [132] M. H. Hamidian, S. D. Edkins, Chung Koo Kim, J. C. Davis, A. P. Mackenzie, H. Eisaki, S. Uchida, M. J. Lawler, E.-A. Kim, S. Sachdev, and K. Fujita, “Atomic-scale electronic structure of the cuprate d -symmetry form factor density wave state,” *Nature Physics* **12**, 150 (2016).
- [133] Kazuhiro Fujita, Mohammad H. Hamidian, Stephen D. Edkins, Chung Koo Kim, Yuhki Kohsaka, Masaki Azuma, Mikio Takano, Hidenori Takagi, Hiroshi Eisaki, Shin ichi Uchida, Andrea Allais, Michael J. Lawler, Eun-Ah Kim, Subir Sachdev, and J. C. Séamus Davis, “Direct phase-sensitive identification of a $i_x i_y d_x^2 - i_y^2$ -form factor density wave in underdoped cuprates,” *Proceedings of the National Academy of Sciences* **111**, E3026–E3032 (2014).
- [134] Wei Zhang, Xinyou Liu, Lingfei Wang, Chun Wai Tsang, Zheyu Wang, Siu Tung Lam, Wenyan Wang, Jianyu Xie, Xuefeng Zhou, Yusheng Zhao, Shanmin Wang, Jeff Tallon, Kwing To Lai, and Swee K. Goh, “Nodeless superconductivity in kagome metal CsV_3Sb_5 with and without time reversal symmetry breaking,” *Nano Letters* **23**, 872 (2023).
- [135] Nyayabanta Swain, Madhuparna Karmakar, and Pinaki Majumdar, “Spin-orbital liquids and insulator-metal transitions on the pyrochlore lattice,” *Phys. Rev. B* **106**, 245114 (2022).
- [136] Madhuparna Karmakar and Nyayabanta Swain, “Transport and spectroscopic signatures of a disorder-stabilized metal in two-dimensional frustrated mott insulators,” *Phys. Rev. B* **105**, 195146 (2022).
- [137] Nyayabanta Swain and Madhuparna Karmakar, “Strain-induced superconductor-insulator transition on a lieb lattice,” *Phys. Rev. Res.* **2**, 023136 (2020).
- [138] Shashikant Singh Kunwar and Madhuparna Karmakar, “Kagome hubbard model away from the strong coupling limit: Flat band localization and non fermi liquid signatures,” (2024), [arXiv:2404.05787 \[cond-mat.str-el\]](https://arxiv.org/abs/2404.05787).
- [139] Santhosh Kannan, Jainam Savla, and Madhuparna Karmakar, “Metal-insulator transition and thermal scales in d -wave altermagnet,” (2026), [arXiv:2603.02707 \[cond-mat.str-el\]](https://arxiv.org/abs/2603.02707).
- [140] Sabyasachi Tarat and Pinaki Majumdar, “A real space auxiliary field approach to the bcs-bec crossover,” *The European Physical Journal B* **88**, 68 (2015).
- [141] Madhuparna Karmakar and Pinaki Majumdar, “Population-imbalanced lattice fermions near the bcs-bec crossover: Thermal physics of the breached pair and fulde-ferrell-larkin-ovchinnikov phases,” *Phys. Rev. A* **93**, 053609 (2016).
- [142] Madhuparna Karmakar, “Thermal transitions, pseudogap behavior, and bcs-bec crossover in fermi-fermi mixtures,” *Phys. Rev. A* **97**, 033617 (2018).
- [143] Rajarshi Tiwari and Pinaki Majumdar, “The crossover from a bad metal to a frustrated mott insulator,” (2013), [arXiv:1301.5026 \[cond-mat.str-el\]](https://arxiv.org/abs/1301.5026).
- [144] Nyayabanta Swain, Rajarshi Tiwari, and Pinaki Majumdar, “Mott-hubbard transition and spin-liquid state on the pyrochlore lattice,” *Phys. Rev. B* **94**, 155119 (2016).
- [145] Nyayabanta Swain and Pinaki Majumdar, “Magnetic order and mott transition on the checkerboard lattice,” *Journal of Physics: Condensed Matter* **29**, 085603 (2017).
- [146] Nyayabanta Swain and Pinaki Majumdar, “Mott transition and anomalous resistive state in the pyrochlore molybdate,” *Europhysics Letters* **119**, 17004 (2017).
- [147] Nyayabanta Swain, Madhuparna Karmakar, and Pinaki Majumdar, “Spin-orbital liquids and insulator-metal transitions on the pyrochlore lattice,” *Phys. Rev. B* **106**, 245114 (2022).
- [148] Matthias Mayr, Gonzalo Alvarez, Cengiz Şen, and Elbio Dagotto, “Phase fluctuations in strongly coupled d -wave superconductors,” *Phys. Rev. Lett.* **94**, 217001 (2005).
- [149] Matthias Mayr, Gonzalo Alvarez, Adriana Moreo, and Elbio Dagotto, “One-particle spectral function and local density of states in a phenomenological mixed-phase model for high-temperature superconductors,” *Phys. Rev. B* **73**, 014509 (2006).
- [150] Anamitra Mukherjee, Niravkumar D. Patel, Adriana Moreo, and Elbio Dagotto, “Orbital selective directional conductor in the two-orbital hubbard model,” *Phys. Rev. B* **93**, 085144 (2016).
- [151] A. I. Buzdin, “Proximity effects in superconductor-ferromagnet heterostructures,” *Rev. Mod. Phys.* **77**, 935–976 (2005).
- [152] Madhuparna Karmakar and Pinaki Majumdar, “Noncollinear order and gapless superconductivity in s -wave magnetic superconductors,” *Phys. Rev. B* **93**, 195147 (2016).
- [153] T. Baba, T. Yokoya, S. Tsuda, T. Kiss, T. Shimojima, K. Ishizaka, H. Takeya, K. Hirata, T. Watanabe, M. Nohara, H. Takagi, N. Nakai, K. Machida, T. Togashi, S. Watanabe, X.-Y. Wang, C. T. Chen, and S. Shin, “Bulk electronic structure of the antiferromagnetic superconducting phase in $\text{ErNi}_2\text{B}_2\text{C}$,” *Phys. Rev. Lett.* **100**, 017003 (2008).
- [154] M. Schneider, G. Fuchs, K.-H. Müller, K. Nenkov, G. Behr, D. Souptel, and S.-L. Drechsler, “Magnetic pair breaking in superconducting $\text{HoNi}_2\text{B}_2\text{C}$ studied on a single crystal by thermal conductivity in magnetic fields,” *Phys. Rev. B* **80**, 224522 (2009).
- [155] Hiroshi Kontani, “Theory of anisotropic s -wave superconductivity with point-node-like gap minima: Analysis of $(\text{Y, Lu})\text{Ni}_2\text{B}_2\text{C}$,” *Phys. Rev. B* **70**, 054507 (2004).
- [156] Roberto Lo Conte, Maciej Bazarnik, Krisztián Palotás, Levente Rózsa, László Szunyogh, André Kubetzka, Kirsten von Bergmann, and Roland Wiesendanger, “Coexistence of antiferromagnetism and superconductivity in $\text{Mn}/\text{Nb}(110)$,” *Phys. Rev. B* **105**, L100406 (2022).
- [157] Stefan Rex, Igor V. Gornyi, and Alexander D. Mirlin, “Majorana bound states in magnetic skyrmions imposed onto a superconductor,” *Phys. Rev. B* **100**, 064504 (2019).
- [158] Guang Yang, Peter Stano, Jelena Klinovaja, and Daniel Loss, “Majorana bound states in magnetic skyrmions,” *Phys. Rev. B* **93**, 224505 (2016).
- [159] Yong Xu, Chunlei Qu, Ming Gong, and Chuanwei Zhang, “Competing superfluid orders in spin-orbit-coupled fermionic cold-atom optical lattices,” *Phys. Rev. A* **89**, 013607 (2014).
- [160] Fan Wu, Guang-Can Guo, Wei Zhang, and Wei Yi, “Unconventional fulde-ferrell-larkin-ovchinnikov pairing states in a fermi gas with spin-orbit coupling,” *Phys. Rev. A* **88**, 043614 (2013).
- [161] M. Iskin, “Trapped fermi gases with rashba spin-orbit coupling in two dimensions,” *Phys. Rev. A* **86**, 065601 (2012).
- [162] M. Iskin and A. L. Subaş ı, “Topological superfluid phases of an atomic fermi gas with in- and out-of-plane zeeman fields and equal rashba-dresselhaus spin-orbit coupling,” *Phys. Rev. A* **87**, 063627 (2013).
- [163] Kangjun Seo, Chuanwei Zhang, and Sumanta Tewari, “Topological uniform superfluid and fulde-ferrell-larkin-ovchinnikov phases in three-dimensional to one-dimensional crossover of spin-orbit-coupled fermi gases,” *Phys. Rev. A* **88**, 063601 (2013).
- [164] Madhuparna Karmakar, “Temperature-tuned fermi-surface topology and segmentation in noncentrosymmetric superconductors,” *Phys. Rev. B* **107**, 064503 (2023).